Food Chemistry 310 (2020) 125977

Contents lists available at ScienceDirect

Food Chemistry

journal homepage: www.elsevier.com/locate/foodchem

A novel route for double-layered encapsulation of probiotics with improved viability under adverse conditions

Kun Feng[a], Ru-meng Huang[a], Rui-qing Wu[a], Yun-shan Wei[a], Min-hua Zong[a], Robert J. Linhardt[b], Hong Wu[a,c,*]

[a] School of Food Science and Engineering, South China University of Technology, Guangzhou 510640, China
[b] Department of Chemical and Biological Engineering, Center for Biotechnology and Interdisciplinary Studies, Rensselaer Polytechnic Institute, Troy, NY 12180, USA
[c] Guangdong Province Key Laboratory for Green Processing of Natural Products and Product Safety, Guangzhou 510640, China

ARTICLE INFO

Keywords:
Lactobacillus plantarum
Coaxial electrospinning
Core-shell structure
Sodium alginate
Survivability

ABSTRACT

To improve the survivability of probiotics under the harsh conditions, a novel double-layered vehicle, which was developed by a one-step coaxial electrospinning procedure, was here used to encapsulate the probiotics. The morphology characterization analysis revealed that the electrospun fiber had a beaded morphology and core-shell structure. Probiotic cells were successfully encapsulated in the fibers (10^7 CFU/mg) and exhibited an oriented distribution along the fiber. Additionally, the encapsulation of core-shell fiber mat enhanced the tolerance of probiotic cells to simulated gastrointestinal conditions and no significant loss of viability was found ($p > 0.05$). Besides that, the encapsulated cells exhibited better thermal stability under heat moisture treatment, lower loss of viability (0.32 log CFU/mL) was occurred when compared with the free cells or encapsulated cells in uniaxial fiber mat. In conclusion, this double-layered vehicle presents a great potential in probiotic encapsulation and improving their resistant ability to the harsh conditions.

1. Introduction

Advances in the biotechnology have promoted the deep understanding of metabolic interactions between the host and microbiome. Recently, increased studies have highlighted the important role of the gut microbiome in regulating the human health and disease (Lee & Hase, 2014). Specifically, the supplementary of probiotics could potentially influence the microbiome composition, and thus conferring several health benefits to the host, such as modulation of immune system, prevention of diarrhea, reduction of lactose intolerance, alleviation of gastrointestinal complaints, etc. (Martinez, Bedani, & Saad, 2015; Sanders et al., 2013; Aureli et al., 2011). However, challenges associated with the consumption of probiotics were existed owing to: (i) harsh food processing and storage conditions (pH, temperature, oxidation content, osmotic pressure, etc.), (ii) harsh gastrointestinal conditions (high acid, digestive enzymes, bile salt, etc.) and (iii) successful colonization in the colon (Tripathi & Giri, 2014; Holkem et al., 2016; Li et al., 2019). To exert their functions, the probiotics should survive the above adverse conditions and maintain a high bacteria survival rate. Herein, microencapsulation has proven to be a promising approach for addressing these challenges.

In recent years, various studies have been performed to investigate the protective role of different encapsulation vehicles against the harsh conditions that to which probiotic cells should be exposed (Šipailienė & Petraitytė, 2018). Specifically, the multilayer structured vehicle has been considered to be more effective in improving the survivability of encapsulated probiotic cells (Laelorspoen, Wongsasulak, Yoovidhya, & Devahastin, 2014; Anselmo, Mchugh, Webster, Langer, & Jaklenec, 2016). However, most of these carriers were hydrogel beads or capsules fabricated by repeated and complex coating process. Therefore, other types of encapsulation vehicles with multilayer structure developed by some simple and new methods are necessary to be explored for protecting the probiotic cells.

Electrospinning, which is a mild and facile technique, has achieved increased interest in bioactive compounds encapsulation (Wen, Zong, Linhardt, Feng, & Wu, 2016). Recently, it was taken as an emerging approach for probiotic encapsulation; however, most studies just preliminarily encapsulated the probiotic cells by uniaxial electrospinning

Abbreviations: SA, sodium alginate; PVA, poly(vinyl alcohol); TEM, transmission electron microscopy; SEM, scanning electron microscopy; ATR-FTIR, attenuated total reflection-Fourier transform infrared spectroscopy; XRD, X-ray diffraction; TGA, thermogravimetric analysis; *L.*, *Lactobacillus*; MRS, de Man-Rogosa-Sharpe; SGF, simulated gastric fluid; SIF, simulated intestinal fluid

* Corresponding author at: School of Food Science and Engineering, South China University of Technology, Guangzhou 510640, China.
E-mail address: bbhwu@scut.edu.cn (H. Wu).

https://doi.org/10.1016/j.foodchem.2019.125977
Received 18 July 2019; Received in revised form 7 November 2019; Accepted 28 November 2019
Available online 04 December 2019

and the ability of the uniaxial fiber mat to help the probiotics to resist the harsh environmental conditions has not been explored yet (Feng et al., 2018; Amna, Hassan, Pandeya, Khil, & Hwang, 2013). In our pretest study, we found that the capability of the obtained uniaxial fiber for protecting the probiotics from the harsh gastric condition was poor and almost all of the cells lost their viability. In regarding to this, coaxial electrospinning is one simple and direct method for developing vehicles with double-layered structure and recent reports have demonstrated that the core-shell electrospun fiber mat has more advantages over uniaxial electrospun fiber in encapsulation and controlled release of drugs (Feng et al., 2019; Yang et al., 2018). However, few studies have been performed on double-layered encapsulation of probiotic cells by coaxial electrospinning and its efficacy in providing protection to the encapsulated probiotic cells under the harsh conditions was unknown. Hence, the double-layer structured vehicle fabricated just through one step by coaxial electrospinning was here considered and we hypothesized that this distinct vehicle maybe a good alternative for encapsulating probiotic cells and conferring protections to them.

Sodium alginate (SA), which is a pH-responsive polymer, was extensively used as the wall material for probiotic encapsulation (Burgain, Gaiani, Linder, & Scher, 2011). But most of the SA-based solid vehicles were fabricated by crosslinking with Ca^{2+} (Li et al., 2018; Li et al., 2017). However, to date, there is no report considering the potential of the SA-based core-shell fiber for probiotic protection. Hence, the aim of this study is to construct a novel double-layered encapsulation vehicle for *Lactobacillus plantarum* (*L. plantarum*) through the one-step coaxial electrospinning procedure. The feasibility of this vehicle for improving their survivability under simulated gastrointestinal conditions and heat moisture treatment was investigated.

2. Materials and methods

2.1. Materials

Sodium alginate (SA, from brown algae) and Rhodamine 123 (≥98%) were from Sigma-Aldrich company (Shanghai, China); Poly (vinyl alcohol) (PVA, 98–98.8% hydrolysis) was purchased from Sinopharm Chemical Reagent Co., Ltd. (Beijing, China); pepsin (3000 U/mg) and trypsin (250 U/mg) were obtained from Aladdin biological technology Co., LTD (Shanghai, China); *L. plantarum* was kindly donated by Prof. Jiguo Yang's laboratory belonging to School of Food Science and Engineering, South China University of Technology.

2.2. Preparation of electrospinning solutions

A tube of stock culture was inoculated into the sterile de broth (MRS) and activated twice at 37 °C. Then the cells were harvested at stationary phase (18 h) by centrifuging at 5000 rpm, 4 °C for 5 min and subsequently washed with sterile water. The obtained cell pellets were then diluted to get a bacterial concentration of 10^{10} CFU/mL by sterile water and then used either for the encapsulation process or the survivability assay.

PVA solutions (6% and 8%, w/w) were prepared by adding PVA into the deionized water and stirred at 80 °C for 2 h with a magnetic stirrer (RT5, IKA, German). SA solution (2%, w/w) was prepared by dissolving SA in deionized water and stirred until complete dissolution for overnight. All the solutions and the glass wares used in this experiment were autoclaved at 121 °C for 15 min to achieve sterility. The shell solution was prepared by blending PVA (8%, w/w) and SA solution at a weight ratio of 80:20. The mixture of 20 μL of cell pellet suspension and 10 g of 6% PVA solution was served as the core solution. The stirring process was performed under sterilized conditions.

2.3. Double-layered encapsulation of probiotic cells by electrospinning

Electrospinning process was carried out by applying a homemade spinneret with two concentric needles (17 gauge and 21 gauge, respectively). The rate of the shell and core solutions were both controlled at 0.4 mL/h by two syringe pumps (NE-300, USA). And the spinneret was connected with the positive electrode of a power supply, which generate a voltage of 16 kV. The prepared fiber was collected at one grounded plate coated with the aluminum foil, the distance between the needle tip and the plate was kept at 14 cm. During the electrospinning process, the temperature and relative humidity were maintained at 25 °C and 40%, respectively.

2.4. Characterization and measurement

The morphologies of the obtained electrospun fiber sample were observed by SEM (EVO18, Germany) at an accelerating voltage of 15 kV. Prior to observation, electrospun fiber mat was coated with Pt for 40 s using a sputter coater (K550, Emitech, UK) under vacuum. Then the distribution of the fiber diameter was analyzed by Nano Measure 1.2 software.

The core-shell structure observation was performed using the TEM (JEM-2010, Japan); electrospun fibers were collected on the copper grid which was previously put on the aluminum foil.

The viability and distribution of probiotic cells were evaluated by fluorescence microscopy. Cells were firstly stained with Rhodamin 123, and then the stained cells encapsulated fiber was fabricated by the method described in Section 2.2. Then a layer of the fiber on the microscope slide was prepared by putting the slide on the aluminum foil before electrospinning. Then the nanofibers containing stained probiotic cells was observed by an inverted fluorescence microscope (IX73, Olympus, Japan), which was fitted with a digital camera (Olympus, Japan). Then the pictures were processed with the Olympus cellSens Standard software.

FTIR spectrophotometer (Bruker Model Equinox 55, Germany) was utilized to investigate the interactions between the components in the obtained fiber mat. ATR-FTIR spectra were recorded using the FTIR spectrometer coupled with an ATR detector. All the measurements were performed in the mid infrared region with a resolution of 4 cm^{-1} and scanning wave number of 500 to 4000 cm^{-1}. The analysis of obtained spectra data was performed by the OPUS spectroscopic software.

The crystal structure of the fiber mat and the relevant constitutes were measured by using an X-ray diffractometer (model D8 Advance, Germany) with a scanning rate of 0.02° per 0.5 s using Cu-Kα radiation. The XRD patterns were obtained in the 2θ range of 5–60°.

The thermal behavior of the fiber mat and the related constituents was investigated using thermal gravimetric analysis (TGA-Q5000, USA). It was carried out at the temperature range from 37 to 700 °C at a heating rate of 10 °C/min under nitrogen atmosphere.

2.5. Survival of free and encapsulated probiotic cells in simulated gastrointestinal condition

In order to fully exert their health benefits to the host, the probiotics should be protected from the destruction of the harsh environment of upper gastrointestinal tract. Therefore, the effectiveness of the core-shell vehicle for the probiotic under simulated acidic and bile condition were investigated. The survival efficiency of the encapsulated cells in the simulate fluids was carried out according to Rajam's methods with some modification (Rajam, Karthik, Parthasarathi, Joseph, & Anandharamakrishnan, 2012).

2.5.1. Survival of encapsulated probiotic cells in simulated gastric condition

The pepsin was dissolved in sterile water (pH 2.0) followed by filtering with a 0.22 μm sterile membrane filter and the simulated gastric fluid (SGF) was prepared by adding the pepsin suspension to the sterile water to get a final concentration of 0.3% (w/v, pH 2.0). 100 mg of the core-shell fiber mat was added into 5 mL SGF and incubated in a shaker incubator (37 °C, 100 rpm) for 2 h. Meanwhile, 100 μL of free cell

suspension was addressed in the same condition and served as the control. After that, the fiber mat or 100 μL of free cell contained solution was harvested from the above SGF, respectively, subsequently transported to the 5 mL of MRS broth and then the microorganisms were activated at 37 °C for 24 h. After that, the medium was spread on the MRS agar plate and incubated at 37 °C for 48 h before colony counting.

2.5.2. Survival of encapsulated probiotic cells in simulated intestinal condition

To examine the bile tolerance of the encapsulated cells, 2% bile salt solution was prepared by adjusting pH to 7.0 with 1 M NaOH and sterilized at 121 °C for 20 min. The trypsin was dissolved in sterile water and filtered. Then the simulated intestinal fluid (SIF) was prepared by suspending trypsin in sterile bile solution (2%, w/w). 100 mg of the core–shell fiber mat or 100 μL of free cell suspension (control) was added into 5 mL SIF and incubated in a shaker incubator (37 °C, 100 rpm) for 2 h. After that, the fiber mat or 100 μL of free cell suspension harvested from the above SIF were transported to 5 mL of MRS broth and then the microorganisms were activated at 37 °C for 24 h. Then the medium was spread on the MRS agar plate and incubated at 37 °C for 48 h before colony counting.

2.6. Thermal stability of free and encapsulated cells

The stability of free and encapsulated cell under heat moisture treatment was carried out according to the previous study (Feng et al., 2018). Briefly, the free cell suspension (control) and the cell loaded core-shell fiber mat were added into the sterile tubes, followed by incubating in the water bath with different temperatures (45 °C, 60 °C, and 70 °C) for 30 min. For the uniaxial fiber mat, its efficacy for protecting the loaded probiotic cell from the moist-heat condition has been investigated in the previous work (Feng et al., 2018). Therefore, in this study, the uniaxial PVA/*L. plantarum* fiber mat was also prepared and processed in the same condition, to compare with the core-shell fiber mat. After the treatment, the cells in different samples were activated in anaerobic atmosphere at 37 °C for 24 h; the numbers of viable cells were then determined as aforementioned in Section 2.4.

2.7. Statistical analysis

The statistical analyses were performed by employing a One-way ANOVA procedure in a SPSS Statistics Software 16.0. All the experiments were carried out in triplicate and resulted data was displayed as mean ± standard deviation. $P < 0.05$ was considered statistically significant.

3. Results and discussion

3.1. Fabrication of the double-layered vehicle

The goal of this study was to construct a suitable carrier to encapsulate the probiotic cells and protect them from the harsh conditions of upper gastrointestinal tract. SA, as a pH-responsive polymer, has been widely used in the field of encapsulation (Alfatama, Lim, & Wong, 2018). However, as an ionic polysaccharide, its application in electrospinning was limited due to its low viscosity and high conductivity. In this regard, the extra polymer should be added to improve the electrospinnability of SA (Safi, Morshed, Ravandi, & Ghiaci, 2007). On basis of our previous study, the fiber with good morphology could be formed by blending the PVA and SA at suitable mass ratio. In this study, the mixture of PVA (8%, w/w) and SA (2%, w/w) with the mass ratio of 4:1 was served as the shell solution and the probiotic cells suspended in 6% (w/w) PVA solution composed the core solution. The scheme of the encapsulation of probiotic cell in nanofibers by coaxial electrospinning was depicted in Scheme 1. The SEM morphology of the obtained fiber was shown in Fig. 1A, it can be seen that the addition of probiotic cells into the spinning solution resulted in beaded fiber morphology, leading to a local widening of the electrospun fiber. Moreover, the beads appeared as approximately oblong and were distributed along the fiber; the similar phenomenon has been reported by previous study (Feng et al., 2018; Fung, Yuen, & Liong, 2011). We hypothesize that the probiotic cells were successfully enclosed within the nanofiber, and more interestingly, the encapsulated cells were oriented in the fiber due to the sink-flow at the Taylor Cone (Dror et al., 2003; Wu et al., 2011). The obtained fiber possessed an average fiber diameter of 270 ± 64 nm, and the collected fiber mat was presented in Fig. 1C. In this study, coaxial electrospinning technique was utilized to develop the core-shell structured fiber to provide the probiotic cells a more protective layer. Herein, TEM was applied to observe the fiber mat since it was a widely used technique for characterizing the core-shell structure (Zhang et al., 2019). The TEM image of the obtained SA/PVA/*L. plantarum* fiber mat was shown in Fig. 1D. It can be seen that the electrospun fiber exhibited an obvious core-shell structure. Besides the SEM, the fluorescence microscopy was further performed to provide the direct evidence that whether the probiotic cells were encapsulated in the core-shell fiber. As depicted in Fig. 1E, the encapsulated cell exhibiting green color were evenly distributed in the electrospun fibers and the oriented distribution phenomenon could be also observed in this figure. Furthermore, as shown in Fig. 1F, the beaded fiber morphology could be clearly seen in the enlarged figure, which further supported the results of the SEM analysis.

3.2. Characterization of the electrospun fiber mat

The possible interactions between the chemical constituents in the fiber mat were examined by ATR-FTIR. The spectra of pure PVA, SA, *L. plantarum*, and SA/PVA/*L. plantarum* fiber mat were depicted in Fig. 2A. The characteristic absorption peak for the PVA, SA and *L. plantarum* appeared at 3471, 3464 and 3418 cm^{-1} was assigned to the stretching vibrations of O—H group (Feng et al., 2017; Larosa et al., 2018). However, the O—H stretching peak in the spectrum of SA/PVA and SA/PVA/*L. plantarum* fiber mats shifted to the lower wavenumber, demonstrating that more hydrogen bonds were formed between SA and PVA. Furthermore, the characteristic peak of SA at the regions of 900–1200 cm^{-1} was attributed to the vibrations of carbohydrate ring. This band also appeared in the spectrum of SA/PVA fiber mat, which provided evidence that the existence of SA in this fiber mat (Tam et al., 2006). The spectrum of *L. plantarum* in the range of 900–1300 cm^{-1} indicated the bacterial proteins and nucleic acids (Shah, Gani, Ahmad, Ashwar, & Masoodi, 2016). For the spectrum of the SA/PVA/*L. plantarum* fiber mat, this region changed greater in intensity and narrower in width and also showed a blue shift, which was in accordance with the previous study (Vodnar, Socaciu, Rotar, & Stanila, 2010), demonstrating the existence of cells in the fibers. Therefore, this result together with the SEM as well the fluorescence microscopy analysis all confirmed that the probiotic cells were successfully encapsulated in the core-shell fiber mat.

The XRD patterns of PVA, SA, *L. plantarum* and SA/PVA/*L. plantarum* fiber mat were displayed in Fig. 2B. For the PVA, it was clearly seen that a significant crystalline peak was existed at around 19.6°, which was attributed to the strong intermolecular and intramolecular hydrogen bonding (Shalumon, Anulekha, Nair, Chennazhi, & Jayakumar, 2011; Zhang et al., 2007). In addition, SA exhibited a sharp crystalline peak at 13.40°, and it was one typical peak of SA that was reported in the previous literature (Rathna, Birajdar, Bhagwani, & Paul, 2013). As shown in the pattern of SA/PVA/*L. plantarum* fiber mat, the intense peak in PVA had a significant influence on the formation of the crystalline nature fiber mat. However, the intensity of the diffraction peak at 19.6° of the pure PVA became lower and broader, thus resulting in a broader peak at 19.86°. The possible reason behind this phenomenon was that the hydrogen-bonding interactions were formed between

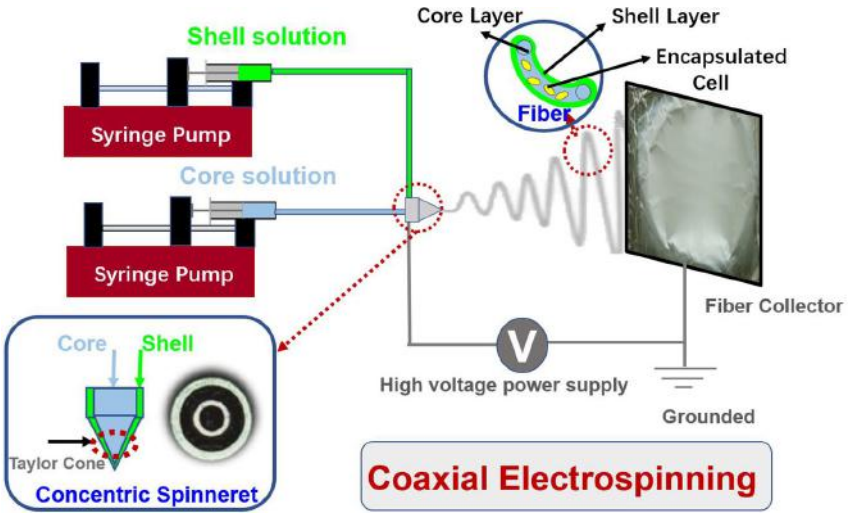

Scheme 1. Procedure for encapsulation of probiotic cells by coaxial electrospinning.

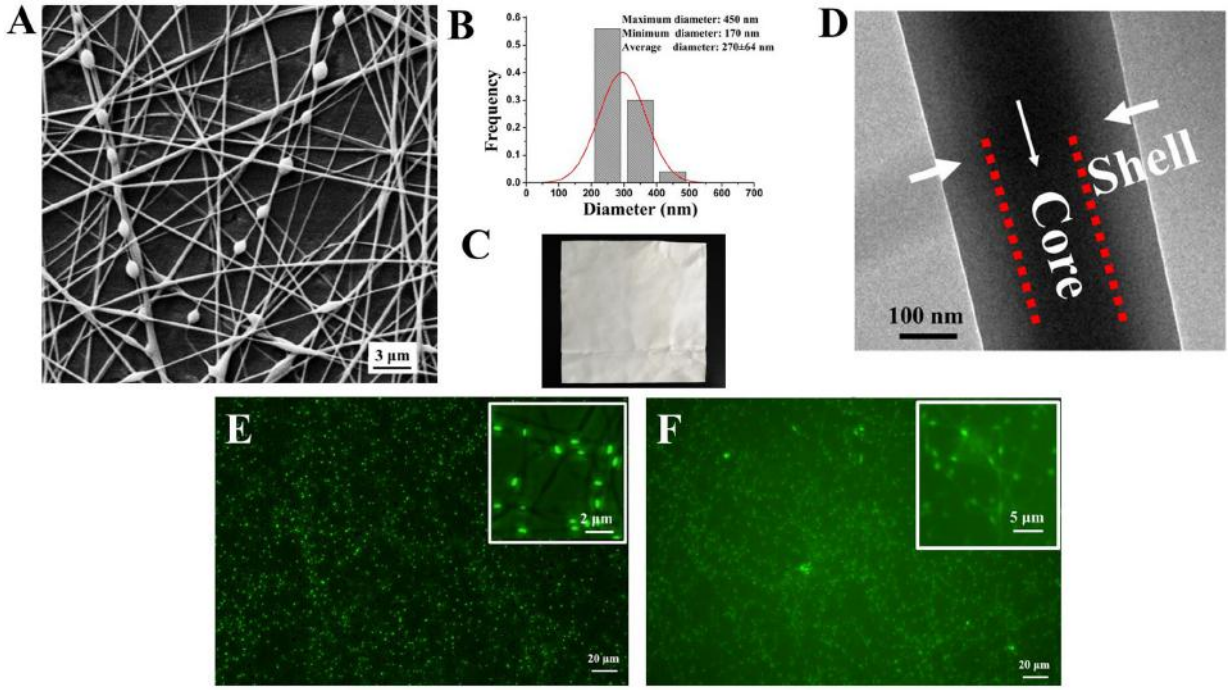

Fig. 1. SEM image (A), fiber diameter distribution (B), photograph (C), TEM image (D) and inverted fluorescence microscopy image (E, F) of the SA/PVA/*L. plantarum* fiber mat.

the carboxyl of hydroxyl groups of SA and the hydroxyl groups of PVA (Islam & Karim, 2010). On the other hand, the broad peak in the core-shell fiber mat indicated the decrease of crystallinity during the electrospinning process; the polymers had less time to crystallize due to the immediately evaporation of solvent and the solidification of the fiber (Rathna et al., 2013). Apart from that, the molecular interactions and crystalline structure of SA were hindered by the added PVA due to the hydrogen-bonding interactions between the PVA and SA, the similar phenomenon was reported by Islam (Islam & Karim, 2010).

The weight loss and related derivate curves of different samples were depicted in Fig. 2. For all the samples, the first degraded stage below 100 °C was attributed to the evaporation of water. As for the TGA curve of SA/PVA/*L. plantarum* fiber mat depicted in Fig. 2C, it degraded mainly in three steps which were evidenced by its DTG curve. Clearly, intensive reaction peaks were presented at 52 °C, 278 °C and 444 °C, respectively. In particular, as shown in Fig. 2D, the second degradation temperature at the maximum degradation percentage for the SA (241 °C) was lower than that of PVA (289 °C). Moreover, it was interesting to see that this temperature for the core-shell fiber mat was lower than that of PVA due to the incorporation of SA. This phenomenon was similar to the previous report and could further demonstrated that the existence of SA in the core-shell fiber mat (Yang, Wang, & Chiu, 2014). Finally, the third degradation step occurred at 400–500 °C was mainly due to the degradation of PVA byproducts which was previously

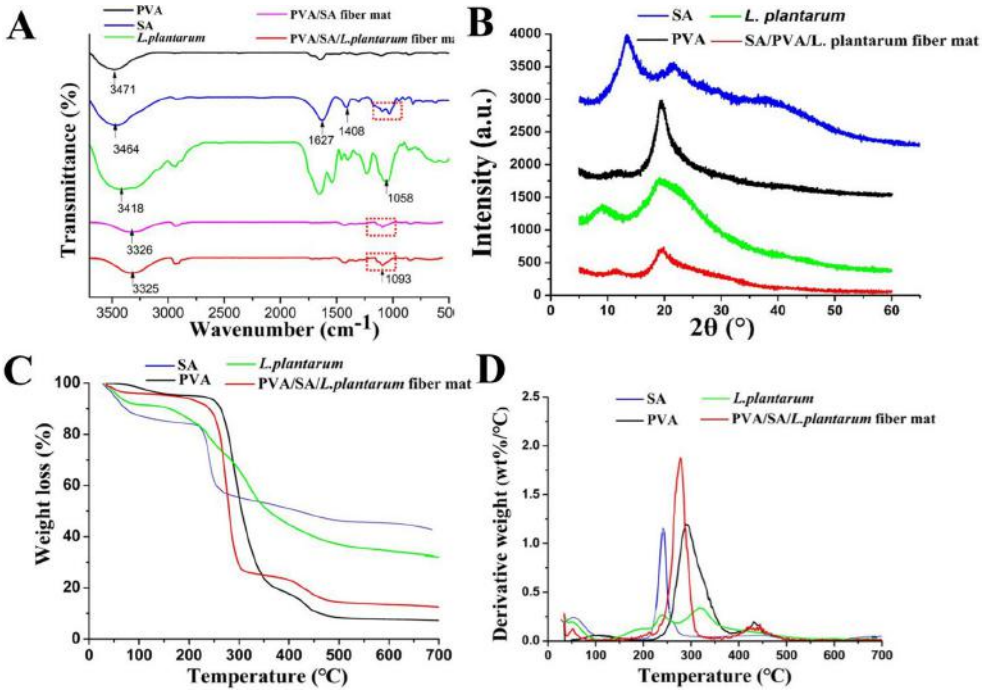

Fig. 2. FTIR spectra, XRD patterns, TGA (A) and DTG (B) curves of different samples.

reported by other study (Chen, Wang, Mao, & Yang, 2007).

3.3. Survival of free and encapsulated probiotic cells in simulated gastric condition

For the encapsulation of probiotic cells, the ability to tolerate the harsh conditions of the upper gastrointestinal tract was an important factor for evaluating the protective efficacy of the obtained vehicles. As for probiotic cell electrospinning, our previous study has approved that the applied voltage had no significant influence on the viability of the encapsulated cell (Feng et al., 2018). However, we found that the encapsulation of probiotic cells in the uniaxial electrospun fiber mat could not help the cells to resist the harsh acid condition and almost all of the cells lost their viability in our preliminary study. Thereby, a novel double-layered encapsulation vehicle for probiotic cells fabricated by a simple coaxial electrospinning was employed to improve the survivability of the loaded cells in the adverse conditions. SA, as a pH responsive polysaccharide, has been utilized for microencapsulation of probiotics and its ability to improve the survivability of the encapsulate cells in SGF has been proved (Tao et al., 2019). Therefore, the double-layered vehicle was prepared with SA as the shell layer, and its efficacy for protecting the encapsulated cells was investigated in this study. The survivability of free and encapsulated cells in SGF was shown in Table 1. It was obviously seen that the free cells (control) suffered a significant loss of viability after exposure to SGF (> 3 log CFU/mL), however, no obvious changes for the viability of encapsulated cells in the core-shell fiber mat was found ($p > 0.05$). The increased SGF tolerance was bestowed by the double-layered encapsulation. In addition, it was known that the growth of probiotic cell could generate short-chain fatty acids and other organic acids, which would result in the decrease of pH value of the MRS broth (Sangalis & Shah, 2010). Hence, the pH values of MRS broth cultured with different samples could from one side reflected the concentration of the probiotic cells. Considering the free and encapsulated cells untreated with SGF, there was no significant for the pH values of the culture media ($P > 0.05$). In particular, the pH of the culture medium for the encapsulated cell treated with SGF displayed a similar value to the untreated group, which was consistent with the result of colony counting. However, the pH value of MRS broth cultured with the treated free cell was obviously higher than other groups, and almost similar to that of the control MRS broth (pH 6.2), indicating the great loss of the viability of free cells due to the destruction of the SGF condition ($P < 0.05$). These results both revealed that the double-layered encapsulation of probiotic cells in the core–shell structured fiber mat conferred protection to the encapsulated cells against the destruction of simulated gastric condition. This was in agreement with other reports, they also proved that the application of SA could improve the survivability of the encapsulated probiotic cells in the simulated gastric condition, while the free cells were absolutely destroyed (Goderska, Zybals, & Czarnecki, 2003; Holkem et al., 2016). In terms of cell encapsulation by SA, hydrogel bead was the widely studied formulation; however, other types of carrier prepared with SA were less explored. Herein, this study preliminarily evaluated the efficiency of the SA based core-shell nanofiber for protecting the encapsulated probiotic cells.

Table 1
Survivability of free cells and encapsulated cells in SA/PVA/*L. plantarum* core-shell fiber mat after exposure to simulated gastric condition.

Sample	No. of viable cells (log CFU/mL)	pH
Encapsulated Cell	9.45 ± 0.3a	3.75 ± 0.03b
Encapsulated Cell (SGF treated)	9.39 ± 0.1a	3.76 ± 0.03b
Free Cell	9.81 ± 0.1a	3.69 ± 0.06b
Free Cell (SGF treated)	NP	6.02 ± 0.02a

Note: Different letters in the individual column indicate the significant difference between each sample tested ($p < 0.05$); NP, not probiotic enumeration (minor than 6 log CFU/mL).

Table 2
Survivability of free cells and encapsulated cells in SA/PVA/*L. plantarum* core-shell fiber mat after exposure to simulated intestinal condition.

Sample	No. of viable cells (log CFU/mL)	pH
Encapsulated Cell	9.45 ± 0.31ab	3.72 ± 0.13b
Encapsulated Cell (SIF treated)	8.39 ± 0.13b	4.35 ± 0.21a
Free Cell	10.42 ± 0.10a	3.66 ± 0.02b
Free Cell (SIF treated)	7.82 ± 0.07c	4.58 ± 0.11a

Note: Different letters in the individual column indicate the significant difference between each sample tested ($p < 0.05$).

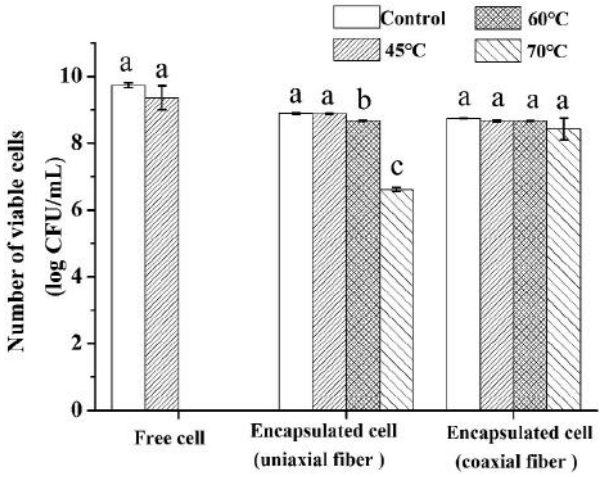

Fig. 3. Survivability of free cells and encapsulated cells in SA/PVA/*L. plantarum* nanofibers after exposure to heat moisture treatments. Values with different letters (a, b, and c) represent significant differences for the samples under different temperatures ($p < 0.05$).

3.4. Survival of free and encapsulated probiotic cells in simulated intestinal condition

To confer the health benefits in the colon, the probiotic cell should avoid the destruction of the harsh condition of upper gastrointestinal tract and reach the colon in enough quantities. Hence, besides the tolerance of encapsulated cells to the SGF, the survival of the encapsulated and free cells in the SIF condition was also essential to investigate. As shown in Table 2, no significant loss of the viability was found for the encapsulated cells after 120 min of incubation in SIF ($p > 0.05$). In contrast, the number of free cells declined significantly during the incubation time, approximately 2.6 log CFU/mL of reduction was observed after exposure to the bile condition. Mandal et al. also reported that the free cells suffered a decrease of 2.2–3.7 log CFU/mL after exposure to the bile sat with different concentration, while the encapsulation of probiotic cell by SA could improve the viability of the encapsulated cell in bile salt (Mandal, Puniya, & Singh, 2006). Additionally, the pH values of the culture media for free and encapsulated cell groups that were treated or untreated with SIF were shown in Table 2. It can be clearly seen that the pH values for all the groups were much less than 6.0, suggesting the proliferation of the probiotic cells.

3.5. Thermal stability of free and encapsulated cells

Besides the adverse digestive condition, the product processing was another crucial factor that would significantly influence the viability of the probiotic cell. As one unit of the food processing, the heat treatment was easily resulted in the loss of viability of probiotic cells. For the probiotic cells, the suitable temperature for growth was at the ranges of 37–43 °C (Tripathi & Giri, 2014). The protection efficiency of the core-shell fiber for the encapsulated cells under the heat moisture treatment was investigated and the free cells were also treated with the same temperature and served as the control. The relevant results were displayed in Fig. 3, and it was noticed that there was no significant change of the viability of free and encapsulated cells treated at 45 °C when compared with the control group. However, the number of the free cell was gradually decreased with the increase of temperature, while the free cells almost lost all of their viability when the temperatures were 60 °C and 70 °C. In our previous study, the encapsulation of *L. plantarum* in the uniaxial fiber mat could protect the cell from the higher temperature and improve its viability to some extent. Hence, in this study, the PVA/*L. plantarum* uniaxial fiber mat was also prepared and its capability for resisting the high temperature was compared with that of the core–shell fiber mat. Results demonstrated that both the uniaxial and core-shell fiber mat could improve the stability of the encapsulated cells under the heat moisture treatment. The viable number of the encapsulated cell treated with 70 °C for 30 min were all above 6 log CFU/mL. However, the probiotic cells encapsulated in core-shell fiber mat suffered a lower loss of viability (0.32 log CFU/mL) than that of encapsulated cell in uniaxial fiber mat (2.28 log CFU/mL), demonstrating that the obtained core-shell fiber mat seems to provide a better protection for the encapsulated probiotic cells.

4. Conclusions

In this study, a novel double-layered encapsulation vehicle was successfully fabricated though a one-step coaxial electrospinning procedure. The resulting electrospun nanofiber showed a beaded morphology and core-shell structure. SEM results indicated that the probiotic cells were successfully encapsulated in the fiber and displayed an oriented distribution along the fiber, which was further confirmed by the results of inverted fluorescent microscopy as well as the FTIR analysis. Additionally, the encapsulation of probiotic cells in the core-shell fiber mat enhanced its tolerance to simulated gastric conditions and no significant loss of viability was found ($p > 0.05$). Apart from that, the thermal stability of encapsulated cells in the core-shell fiber mat under the heat moisture treatment was obviously better than those of the free cells or the encapsulated cells in the uniaxial fiber mat. Therefore, the obtained results confirmed that this core-shell fiber mat was a promising vehicle for encapsulating probiotic cells and conferring protections to them. This study could not only provide an alternative approach for the encapsulation of probiotics, but further promote the application of electrospinning technique in the field of food industry.

Declaration of Competing Interest

The authors declare that they have no known competing financial interests or personal relationships that could have appeared to influence the work reported in this paper.

Acknowledgements

We acknowledge the Science and Technology Project of Guangzhou City (No. 201804010151), the Natural Science Foundation of Guangdong Province (No. 2017A030313148) and the National Natural Science Foundation of China (No. 31671852) for financial support.

References

Alfatama, M., Lim, L. Y., & Wong, T. W. (2018). Alginate-C18 conjugate nanoparticles loaded in tripolyphosphate-crosslinked chitosan-oleic acid conjugate-coated calcium alginate beads as oral insulin carrier. *Molecular Pharmaceutics, 15*, 3369–3382.

Amna, T., Hassan, M. S., Pandeya, D. R., Khil, M. S., & Hwang, L. H. (2013). Classy non-wovens based on animate *L. gasseri*-inanimate poly(vinyl alcohol): Upstream application in food engineering. *Applied Microbiology and Biotechnology, 97*(10),

4523–4531.
Anselmo, A. C., Mchugh, K. J., Webster, J., Langer, R., & Jaklenec, A. (2016). Layer-by-Layer encapsulation of probiotics for delivery to the microbiome. *Advanced Materials, 28*(43) 9442–9442.
Aureli, P., Capurso, L., Castellazzi, A. M., Clerici, M., Giovannini, M., Morelli, L., et al. (2011). Probiotics and health: An evidence-based review. *Pharmacological Research, 63*, 366–376.
Burgain, J., Gaiani, C., Linder, M., & Scher, J. (2011). Encapsulation of probiotic living cells: From laboratory scale to industrial applications. *Journal of Food Engineering, 104*(4), 467–483.
Chen, C. H., Wang, F. Y., Mao, C. F., & Yang, C. H. (2007). Studies of chitosan. I. Preparation and characterization of chitosan/poly(vinyl alcohol) blend films. *Journal of Applied Polymer Science, 105*(3), 1086–1092.
Dror, Y., Salalha, W., Khalfin, R. L., Cohen, Y., Yarin, A. L., & Zussman, E. (2003). Carbon nanotubes embedded in oriented polymer nanofibers by electrospinning. *Langmuir, 19*(17), 7012–7020.
Feng, K., Li, C., Wei, Y. S., Zong, M. H., Wu, H., & Han, S. Y. (2019). Development of a polysaccharide based multi-unit nanofiber mat for colon-targeted sustained release of salmon calcitonin. *Journal of Colloid and Interface Science, 552*, 186–195.
Feng, K., Wen, P., Yang, H., Lou, W. Y., Li, N., Zong, M. H., et al. (2017). Enhancement of the antimicrobial activity of cinnamon essential oil-based electrospun nanofilm by incorporation of lysozyme. *RSC Advances, 7*, 1572–1580.
Feng, K., Zhai, M. Y., Zhang, Y., Linhardt, R. J., Zong, M. H., Li, L., et al. (2018). Improved viability and thermal stability of the probiotics encapsulated in a novel electrospun fiber mat. *Journal of Agricultural and Food Chemistry, 66*(41), 10890–10897.
Fung, W. Y., Yuen, K. H., & Liong, M. T. (2011). Agrowaste-based nanofibers as a probiotic encapsulant: Fabrication and characterization. *Journal of Agricultural and Food Chemistry, 59*(15), 8140–8147.
Goderska, K., Zybals, M., & Czarnecki, Z. (2003). Characterization of microencapsulated *Lactobacillus rhamnosus* LR7 strain. *Polish Journal of Food and Nutrition Science, 12*(53), 21–24.
Holkem, A. T., Raddatz, G. C., Nunes, G. L., Cichoski, A. J., Jacob-Lopes, E., Grosso, C. R. F., et al. (2016). Development and characterization of alginate microcapsules containing *Bifidobacterium* BB-12 produced by emulsification/internal gelation followed by freeze drying. *LWT – Food Science and Technology, 71*, 302–308.
Islam, M. S., & Karim, M. R. (2010). Fabrication and characterization of poly(vinyl alcohol)/alginate blend nanofibers by electrospinning method. *Colloids and Surfaces A-Physicochemical and Engineering Aspects, 366*(1), 135–140.
Laelorspoen, N., Wongsasulak, S., Yoovidhya, T., & Devahastin, S. (2014). Microencapsulation of *Lactobacillus acidophilus* in zein–alginate core–shell microcapsules via electrospraying. *Journal of Functional Foods, 7*, 342–349.
Larosa, C., Salerno, M., de Lima, J. S., Meri, R. M., da Silva, M. F., da Carvalho, L. B., et al. (2018). Characterisation of bare and tannase-loaded calcium alginate beads by microscopic, thermogravimetric, FTIR and XRD analyses. *International Journal of Biological Macromolecules, 115*, 900–906.
Lee, W. J., & Hase, K. (2014). Gut microbiota-generated metabolites in animal health and disease. *Nature Chemical Biology, 10*(6), 416–424.
Li, Z., Behrens, A. M., Ginat, N., Tzeng, S. Y., Lu, X. G., Sivan, S., et al. (2018). Biofilm-inspired encapsulation of probiotics for the treatment of complex infections. *Advanced Materials, 30*(51), 1803925.
Li, C., Bei, T. T., Niu, Z. H., Guo, X., Wang, M. S., Lu, H. Q., et al. (2019). Adhesion and colonization of the probiotic *Lactobacillus rhamnosus* labeled by dsred2 in mouse gut. *Current Microbiology, 76*(7), 896–903.
Li, Y., Feng, C., Li, J., Mu, Y. Z., Liu, Y., Kong, M., et al. (2017). Construction of multilayer alginate hydrogel beads for oral delivery of probiotics cells. *International Journal of Biological Macromolecules, 105*(part 1), 924–930.
Mandal, S., Puniya, A. K., & Singh, K. (2006). Effect of alginate concentrations on survival of microencapsulated *Lactobacillus casei* NCDC-298. *International Dairy Journal, 16*(10), 1190–1195.
Martinez, R. C. R., Bedani, R., & Saad, S. M. I. (2015). Scientific evidence for health effects attributed to the consumption of probiotics and prebiotics: An update for current perspectives and future challenges. *British Journal of Nutrition, 114*(12), 1993–2015.
Rajam, R., Karthik, P., Parthasarathi, S., Joseph, G. S., & Anandharamakrishnan, C. (2012). Effect of whey protein–alginate wall systems on survival of microencapsulated *Lactobacillus plantarum* in simulated gastrointestinal conditions. *Journal of Functional Foods, 4*(4), 891–898.
Rathna, G. V. N., Birajdar, M. S., Bhagwani, M., & Paul, V. L. (2013). Studies on fabrication, characterization, and metal extraction using metal chelating nonwoven nanofiber mats of poly(vinyl alcohol) and sodium alginate blends. *Polymer Engineering and Science, 53*(2), 321–333.
Safi, S., Morshed, M., Ravandi, S. A. H., & Ghiaci, M. (2007). Study of electrospinning of sodium alginate, blended solutions of sodium alginate/poly(vinyl alcohol) and sodium alginate/poly(ethylene oxide). *Journal of Applied Polymer Science, 104*(5), 3245–3255.
Sanders, M. E., Guarner, F., Guerrant, R., Holt, P. R., Quigley, E. M., Sartor, R. B., et al. (2013). An update on the use and investigation of probiotics in health and disease. *Gut, 62*(5), 787–796.
Sangalis, D., & Shah, N. P. (2010). Metabolism of oligosaccharides and aldehydes and production of organic acids in soymilk by probiotic bifidobacterial. *International Journal of Food Science and Technology, 39*(5), 541–554.
Shah, A., Gani, A., Ahmad, M., Ashwar, B. A., & Masoodi, F. A. (2016). β-Glucan as an encapsulating agent: Effect on probiotic survival in simulated gastrointestinal tract. *International Journal of Biological Macromolecules, 82*, 217–222.
Shalumon, K. T., Anulekha, K. H., Nair, S. V., Chennazhi, K. P., & Jayakumar, R. (2011). Sodium alginate/poly(vinyl alcohol)/nano ZnO composite nanofibers for antibacterial wound dressings. *International Journal of Biological Macromolecules, 49*(3), 247–254.
Šipailienė, A., & Petraitytė, S. (2018). Encapsulation of probiotics: Proper selection of the probiotic strain and the influence of encapsulation technology and materials on the viability of encapsulated microorganisms. *Probiotics and Antimicrobial Proteins, 10*(1), 1–10.
Tam, S. K., Dusseault, J., Polizu, S., Menard, M., Halle, J. P., & Yahia, L. (2006). Physicochemical model of alginate–poly-L-lysine microcapsules defined at the micrometric/nanometric scale using ATR-FTIR, XPS, and ToF-SIMS. *Biomaterials, 26*(34), 6950–6961.
Tao, T., Ding, Z., Hou, D. P., Prakash, S., Zhao, Y. N., Fan, Z. P., et al. (2019). Influence of polysaccharide as co-encapsulant on powder characteristics, survival and viability of microencapsulated *Lactobacillus paracasei* Lpc-37 by spray drying. *Journal of Food Engineering, 252*, 10–17.
Tripathi, M. K., & Giri, S. K. (2014). Probiotic functional foods: Survival of probiotics during processing and storage. *Journal of Functional Foods, 9*(9), 225–241.
Vodnar, D. C., Socaciu, C., Rotar, A. M., & Stanila, A. (2010). Morphology, FTIR fingerprint and survivability of encapsulated lactic bacteria (*Streptococcus thermophilus and Lactobacillus delbrueckii subsp. bulgaricus*) in simulated gastric juice and intestinal juice. *International of Food Science and Technology, 45*(11), 2345–2351.
Wen, P., Zong, M. H., Linhardt, R. J., Feng, K., & Wu, H. (2016). Electrospinning: A novel nano-encapsulation approach for bioactive compounds. *Trends in Food Science and Technology, 70*, 56–68.
Wu, D. F., Shi, T. J., Yang, T., Sun, Y. R., Zhai, L. F., Zhou, W. D., et al. (2011). Electrospinning of poly(trimethylene terephthalate)/carbon nanotube composites. *European Polymer Journal, 47*(3), 284–293.
Yang, J. M., Wang, N. C., & Chiu, H. C. (2014). Preparation and characterization of poly (vinyl alcohol)/sodium alginate blended membrane for alkaline solid polymer electrolytes membrane. *Journal of Membrane Science, 457*, 139–148.
Yang, Y. Y., Liu, Z. P., Yu, D. G., Wang, K., Liu, P., & Chen, X. H. (2018). Colon-specific pulsatile drug release provided by electrospun shellac nanocoating on hydrophilic amorphous composites. *International Journal of Nanomedicine, 13*, 2395–2404.
Zhang, Y. B., Zhang, Y., Zhu, Z., Jiao, X. Y., Shang, Y. L., & Wen, Y. Q. (2019). Encapsulation of thymol in biodegradable nanofiber via coaxial eletrospinning and applications in fruit preservation. *Journal of Agricultural and Food Chemistry, 67*(6), 1736–1741.
Zhang, Y. Y., Huang, X. B., Duan, B., Wu, L. L., Li, S., & Yuan, X. Y. (2007). Preparation of electrospun chitosan/poly(vinyl alcohol) membranes. *Colloid Polymer Science, 285*(8), 855–863.